International Journal of ChemTech Research
CODEN (USA): IJCRGG ISSN: 0974-4290
Vol.7, No.4, pp 1930-1937, 2014-2015

# Effect of Divalent Metal Dopant on the Structural and optical Properties of $Tio_2$ Quantum Dots

**S.Chitra[1]*, D. Easwaramoorthy[2]**

[1]Department of Chemistry, Jeppiaar Engineering College, Chennai, India
[2]Department of Chemistry, B.S. Abdur Rahman University, Chennai, India

**Abstract:** In search of efficient materials for photo anode for DSSC, we made an attempt to prepare pure and transition metal ($Zn^{2+}$, $Cd^{2+}$ and $Ni^{2+}$) doped $Tio_2$ simple microwave irradiated solvothermal method. The samples were characterized by structural and optical measurements. The particle size increased as the addition of dopant in the host $TiO_2$ lattices was increased in accordance with the crystallite size obtained by XRD analysis.UV-Vis spectral measurement suggests that addition of dopants in the host $TiO_2$ lattices helping to tune the optical band gap energy.The presence of small amount of dopants (5 mole % of $Zn^{2+}$, $Cd^{2+}$ and $Ni^{2+}$) greatly affects the PL intensity of thehost $TiO_2$ nanocrystals. The doped nanocrystals($TiO_2$:$Zn^{2+}$, $TiO_2$:$Cd^{2+}$ and $TiO_2$:$Ni^{2+}$) leads to strong enhancement in photoluminescence yield compared to pure $TiO_2$ and consequently to new useful materials for photonic applications.
**Keywords:** Solarcell, SEM,TEM, W-H PLOT, Crystallite size , Band gap, Photocondu-ctivity.

## 1. Introduction

It is well known that semiconductors with nanostructures, such as nanowires, nanorods, nanotubes, nanobelts and so on are fascinating due to their novel photoelectrical properties and the unique quantum effects related to the material architectures [1-3].Titanium dioxide($TiO_2$) as one of the most promising photo catalysts has many advantages such as chemical stability, easy availability, energy-saving and non-toxicity, which make it attractive for the photochemical production of hydrogen and wastewater treatments[4-6]. $TiO_2$ is emerging as an attractive material because of its surface photochemistry as well as peculiar chemical and physical behaviours. But the band gap of $TiO_2$ (3.0 – 3.2 eV) is too wide to absorb the visible light efficiently, which leads to some limitations for the practical applications. Many efforts have been made to extend the visible light response of $TiO_2$, such as metal and non-metal doping [7,8], external dye sensitization [9] or coupling with a narrow band gap semiconductor with a more negative conduction band level [10]. So far, considerable interest has been attracted on doping of $TiO_2$ nanomaterials with fifth main group elements such as Nb, Ta doped $TiO_2$ have been studied as the photoanodes of dye-sensitized solar cells(DSSCs) and showed an improved energy conversion efficiency [11,12]. The modification of $TiO_2$ by means of metal doping can affect the crystallization process, influencing the photocurrent deficiency of DSSCs.Searching on alternative photoanode materials for dye-sensitized solar cells (DSSCs) we made an attempt to modify the properties of TiO2 by adding $Zn^{2+}$, $Cd^{2+}$ and $Ni^{2+}$in 5 mole %. Because Zn and Ni doped $SnO_2$, respectively, have a high power conversion efficiency of up to 4.2% and 3.6%, higher than that of undoped $SnO_2$ which is 3.2% and the reason for this difference is that the Zn and Ni-doped films exhibit an elevated electron Fermi level, which may enhance band bending to lower the density of empty trap states.

## 2. Materials and Methods

The precursor materials such as Titanium tetra chloride ($TiCl_4$), Urea ($CO(NH_2)_2$), Zinc chloride ($ZnCl_2$), Cadmium chloride($CdCl_2$), Nickelchloride($NiCl_2{\cdot}6H_2O$), Ethylene glycol ($C_2H_6O_2$) etc., used for the preparation of pure and doped $TiO_2$ quantum dots were of analytical reagent gradepurity and used as purchased from Aldrich and Merc India without additional purification. Double distilled water and Acetone ($(CH_3)_2CO$) was used to remove any unreacted reactants and unwanted organic byproducts present in the synthesized nanocrystalline materials.

For preparation of pure $TiO_2$ nanocrystals, 0.6 mole CO $(NH_2)_2$was dissolved in 50 ml ethylene glycol under vigorous stirring condition for 1 hour at room temperature. Subsequently 0.2 mole$TiCl_4$solution was added in 50 ml ethylene glycol and then added slowly into the above solution. This solutionwas stirred for another 1 hour at 60 ºC temperature to get a clear and deep blue in colour solution. The resulting dissolved mixture is called as stock solution.

The stock solution was kept in a domestic microwave oven (LG model number LG MH2046HB operated with frequency 2.45 GHz and power 800W). Microwave irradiation was carried out at 30% of maximum power until the solvent gets evaporated completely. The resultant product obtained in the form of colloidal precipitate was cooled to room temperature naturally and centrifuged several times with doubly distilled water and then with acetone to remove the unreacted reactants and organic impurities present in the colloidal precipitate. Then the centrifuged final product was collected and then dried in an oven at 60 ºC for 10 hour and collected as the yield. 5 mole % $ZnCl_2$, $CdCl_2$ and $NiCl_2$was added separately to the stocksolution in the case of preparing $TiO_2$:$Zn^{2+}$, $TiO_2$:$Cd^{2+}$and $TiO_2$:$Ni^{2+}$nanocrystals respectively using a procedure as similar to the above.

All the prepared samples were annealed to 600$^o$Cand used for characterization. Powder X-ray diffraction pattern of the prepared samples were studied with a PANalytical X-ray powder diffractometer with scintillation counter and monochromated Cu $K_\alpha$ ($\lambda$ = 1.54056 Å) radiation. The samples were scanned over the range 20 - 80° at a rate of 1°/min and the step size was 0.02°.Microstructural analysis has been performed using SEM Zeiss-SUPRA 40 by secondary electron imaging mode. The particle size analysis of the as-synthesized material has been carried out using TEM- FEI Technai $G^2$300 kV. Energy dispersive X-ray analysis (EDAX) was used to estimate the composition of the materials using EDX-System OXFORD INCA Energy 200. Optical absorption measurements were done at room temperature using a SHIMADZU UV-2400 PC spectrometer with a medium scan speed sampling interval of 0.5 nm in the wavelength range of 190-1100 nm. The photoluminescence (PL) spectra were obtained on a FLUOROLOG-FL3-11 Spectroflorometer with wavelength resolution of 0.5 nm at room temperature. Xenon arc lamp of 450 W was used as the excitation light source. All the PL spectra in this study were acquired at an excitation wavelength of 300 nm. In photoconductivity study, a Hg bulb of 300 W was used as a photo-excitation source. The time-resolved rise and decay of photocurrent spectra are recorded using RISH Multi 15S with adapter RISH Multi SI-232. The observations have been made at room temperature in ambient air.

## 3. Results and Discussion

### 3.1 Structural Properties

#### 3.1.1 PXRD Analysis

The typical X-ray diffraction patterns of pure and $Zn^{2+}$, $Cd^{2+}$ and $Ni^{2+}$doped $TiO_2$nanocrystals are shown in Figure 1. The pronounced diffraction peaks in the XRD patterns are indexed with the standard JCPDS file no. 89-4921. The specific crystallographic planes confirmed that the formations of the $TiO_2$ tetragonal (anatase) phase with space group $I4_1/amd$. It is evident from the XRD data that there are no extra peaks corresponding to zinc, cadmium and nickel or its related phase like metallic zinc/cadmium/nickel, zinc/cadmium/nickel oxides or any binary zinc/cadmium/nickel phases in the zinc/cadmium/nickel doped $TiO_2$ nanocrystals. Thus, excluding the formation of impurities and confirming that $Zn^{2+}$/$Cd^{2+}$/$Ni^{2+}$ ions were effectively substituted $Ti^{2+}$ sites within $TiO_2$ lattice without affecting the crystal structure of the parent $TiO_2$ compound. The calculated lattice parameters of pure and doped TiO2 nanocrystals are given in Table 1.

**Table 1: Calculated lattice parameters for pure and different dopant added $TiO_2$ nanocrystals (*JCPDS file no. 89-4921)**

| Sample name | Lattice parameter (Å) | | Unit cell volume Å$^3$ |
|---|---|---|---|
| | a=b | c | |
| *$TiO_2$ (anatase) | 3.777 | 9.501 | 135.54 |
| Pure $TiO_2$ | 3.7684 | 9.4796 | 134.61 |
| $TiO_2$:$Zn^{2+}$ | 3.8016 | 9.4643 | 136.77 |
| $TiO_2$:$Cd^{2+}$ | 3.8236 | 9.4370 | 137.96 |
| $TiO_2$:$Ni^{2+}$ | 3.7747 | 9.5063 | 135.45 |

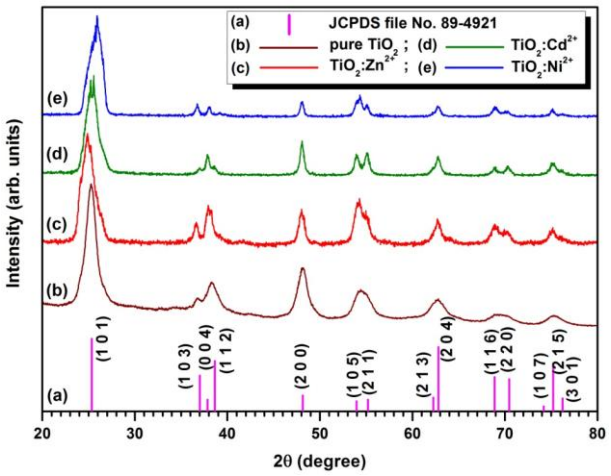


**Figure 1: Powder XRD patterns of pure and doped $TiO_2$nanocrystals annealed at 600 ºC temperatures**

Moreover the higher intensity peak positions ((1 0 1), (1 1 2) and (2 0 4)) of doped $TiO_2$ nanocrystals are slightly shifted into lower or higher angle side. Thus the crystallite size and volume of the unit cells are slightly changed. This reveals that the dopants$Zn^{2+}$/$Cd^{2+}$/$Ni^{2+}$are incorporated into the host $TiO_2$ lattices.The average crystallite sizes of all the synthesized nanocrystals considered in the present study was calculated by using Debye–Scherrer equation and Williamson–Hall plot. The calculated crystallite sizes along with internal strain are given in Table 2.

**Table 2: Calculated crystallite size and lattice strain for pure and doped $TiO_2$ nanocrystals from Scherrer formula and W-H plots**

| Sample name | Crystallite size (nm) | | Lattice strain from W-H plot |
|---|---|---|---|
| | From Scherrer (±0.32 nm) | From W-H plots (±0.19 nm) | x $10^{-3}$ |
| Pure $TiO_2$ | 3.11 | 3.22 | 0.134 |
| $TiO_2$:$Zn^{2+}$ | 4.54 | 4.53 | 0.051 |
| $TiO_2$:$Cd^{2+}$ | 5.41 | 5.14 | -0.717 |
| $TiO_2$:$Ni^{2+}$ | 3.93 | 3.66 | -1.363 |

The cell volume is increasing when $Zn^{2+}$/$Cd^{2+}$/$Ni^{2+}$is assigned to replace Ti sites. In spite of the decrease in 'c', the overall cell volume has never been observed to drop. If directional growth occurs during substitution, the lattice parameter decreases in one direction would be compromised by the increased lattice in other direction.

Therefore it is logical to presume that the lattice growth is more towards 'a' direction than 'c' direction.This nice trend of almost uniform cell volume expansion reveals the dopants $Zn^{2+}$/$Cd^{2+}$/$Ni^{2+}$incorporated into the host $TiO_2$ lattices. In the case of pure $TiO_2$ unit cell volume contraction is takes place when compared to bulk $TiO_2$. This may be due to our synthesized $TiO_2$ nano crystals has lesser crystallite size than that of the bulk material.

### 3.1.2. SEM Analysis

Apart from the crystal structure and crystallite size analysis, yet another important structural characteristic of nanomaterials relates to the gross structural/morphological properties.SEM images were recorded for pure and doped $TiO_2$ nanocrystals. The morphology of pure and doped $TiO_2$ nanocrystals at different dopants ($Zn^{2+}$/$Cd^{2+}$/$Ni^{2+}$) is presented in Figure 2. The spherical nanoparticles are agglomerated so as to reduce the total surface free energy. This evidence always occurs when the particles are small [13]. In this study, the particle size increased as the addition of dopant in the host $TiO_2$ lattices was increased in accordance with the crystallite size obtained by XRD analysis

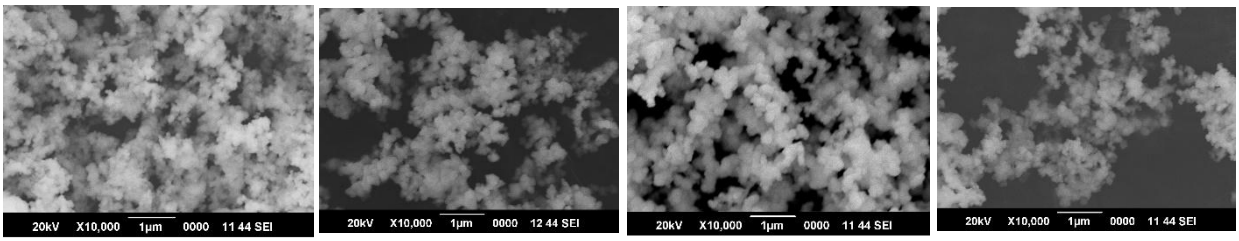


**Figure 2: SEM Images of Pure, $Zn^{2+}$, $Cd^{2+}$and $Ni^{2+}$ doped $TiO_2$ nano crystals**

### 3.1.3 TEM Analysis

TEM images were recorded for pure and doped ($Zn^{2+}$, $Cd^{2+}$ and $Ni^{2+}$)$TiO_2$ nanocrystals. The images are shown in Figure 3. The morphologies of all the samples are found to be nearly spherical in nature with the diameters ranging from 4 to 7 nm. It clearly shows that the average particle size of these spherical samples is nanoscale. It also supports the result of SEM analysis.

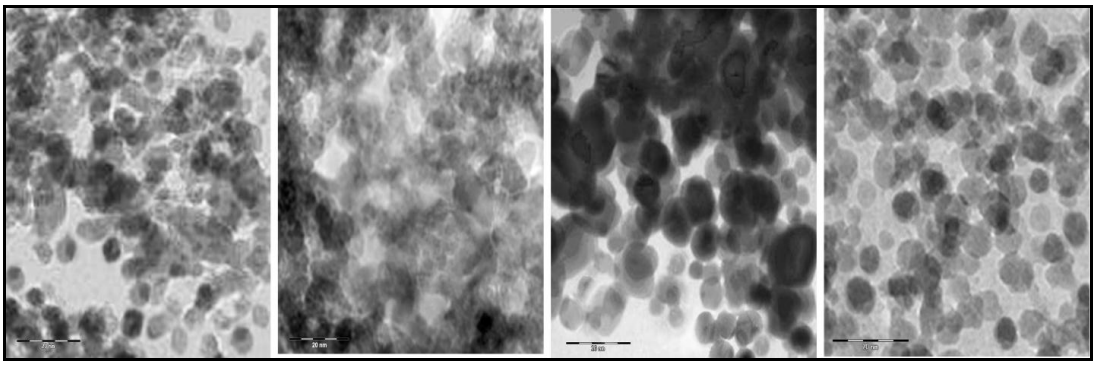

**Figure 3: TEM Images of Pure,$Zn^{2+}$, $Cd^{2+}$and $Ni^{2+}$ doped $TiO_2$nano crystals**

### 3.2 Optical Properties

### 3.2.1 UV-Vis-spectral measurement

UV-Vis absorption spectra were recorded for pure and doped ($Zn^{2+}$, $Cd^{2+}$ and $Ni^{2+}$)$TiO_2$ nanocrystals in the absorbance wavelength range of 200–1200 nm. The recorded spectra are shown in Figure 4a. The absorption data were analyzed and the band gap was estimated using the Tuac's relationship between the absorption coefficient (α) and the photon energy (hυ) [14]. The excitonic absorption peak for pure $TiO_2$ (anatase phase) nanocrystal is

observed at 374 nm (3.318 eV). This is lower than the band gap wavelength of 388 nm (3.2 eV) for bulk $TiO_2$(anatase phase)crystal[15].Figure 4b shows the plots of $(\alpha h\upsilon)^2$ *vs* $h\upsilon$ for pure $TiO_2$, $Zn^{2+}$, $Cd^{2+}$ and $Ni^{2+}$ doped $TiO_2$ nanocrystals. The linear variation of $(\alpha h\upsilon)^2$ *vs* $h\upsilon$ at the absorption edge, confirmed the semiconducting behavior of the prepared nanocrystalswith direct band gap energy [16]. Extrapolating the straight line portion of the plot $(\alpha h\upsilon)^2$ versus $h\upsilon$ for zero absorption coefficient value gives the optical band gap ($E_g$).

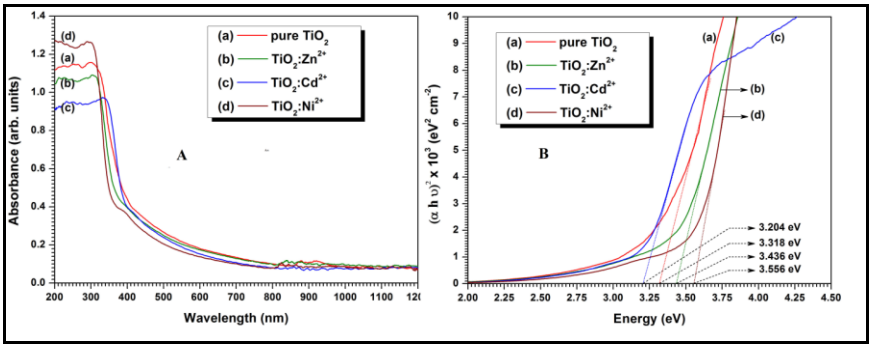


**Figure 4: A) UV-Vis absorption spectra and B) Tauc plot for pure and doped $TiO_2$ nanocrystals**

The substitution of $Zn^{2+}$ and $Ni^{2+}$ in $Ti^{2+}$ sites, the excitonic absorption peak leads to shift in lower wavelength side (blue shift). Whereas in the case of $Cd^{2+}$ substituted $Ti^{2+}$ sites, the excitonic absorption peak leads to shift in higher wavelength side (red shift).The shifting of band gap towards lower/higher energy value (red/blue shift) confirms the dopant entered into the host $TiO_2$ lattices. It suggests that addition of dopants in the host $TiO_2$ lattices helping to tune the optical band gap energy. Our optical band gap energy calculation suggests, for the fabrication of any optical devices which require optical band gap ranging from a minimum of 3.204 eV to maximum 3.556 eV.It may be suggested that the variation in energy band gap will be suitable for window material for fabrication of solar cells.

### 3.2.2 Photoluminescence Analysis

The PL emission spectra of the pure $TiO_2$ and 5 mole % $Zn^{2+}$, $Cd^{2+}$ and $Ni^{2+}$doped $TiO_2$nanocrystals excited at a wavelength of 300 nm at room temperature areshown in Figure 5. From the figure it showed a strong PL emission band around 376 nm (band-edge luminescence band) and a broad emission band ranging from 400 to 550 nm (defect-state luminescence band) for pure $TiO_2$ nanocrystals.The first band arises from the radioactive annihilation of excitons between valance band and conduction band (band-to-band recombination).While the second band (defect-state luminescence band) is attributed to the electron transition mediated by defect levels such as oxygen vacancies in the band gap [17]. Similar behavior was obtained for the doped $TiO_2$ nanocrystals. However the positions of band edge and defect-state luminescence bands were slightly sifted towards lower wavelength side (blue shift) for $TiO_2$:$Zn^{2+}$ and $TiO_2$:$Ni^{2+}$ nanocrystals and higher wavelength side (red shift) for $TiO_2$:$Cd^{2+}$ nanocrystals. The broad visible light emission band for $TiO_2$ nanocrystals is shifted from458 nm (violet emission, 2.70 eV) to 484 nm (bluish emission, 2.56 eV) for $Cd^{2+}$ doped $TiO_2$nanocrystals. In the case of $Zn^{2+}$ and $Ni^{2+}$ doped $TiO_2$ nanocrystals the broad visible light emission bands are slightly blue shifted. This significant red/blue shift provides clear evidence for the formation ofthe dopednanocrystals($TiO_2$:$Zn^{2+}$, $TiO_2$:$Cd^{2+}$ and $TiO_2$:$Ni^{2+}$) rather than forming separate ZnO, CdO, NiO or a mixed phase structured nanocrystals.

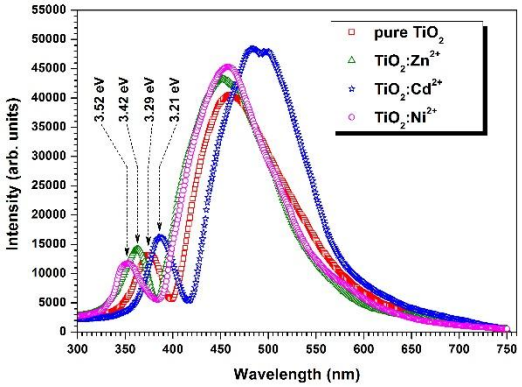


**Figure 5: Photoluminescence emission spectra of pure and doped $TiO_2$ nanocrystals**

### 3.3Photoconductivity properties

The variation of field dependence dark current ($I_d$) and photocurrent ($I_p$) with applied voltage (V) for pure and doped (Zn, Cd and Ni)$TiO_2$ are shown in Figure 6. It is observed that both dark and photo currents of pure and doped $TiO_2$ nano crystals increase linearly with the applied voltage. The photocurrent of both pure and doped $TiO_2$ nanocrystals is more than the dark current, which is termed as positive photoconductivity. All the synthesized pure and doped $TiO_2$nanocrystals considered in the present study are found to exhibit positive photoconductivity. This may be attributed to the generation of mobile charge carriers caused by absorption of photons [18].

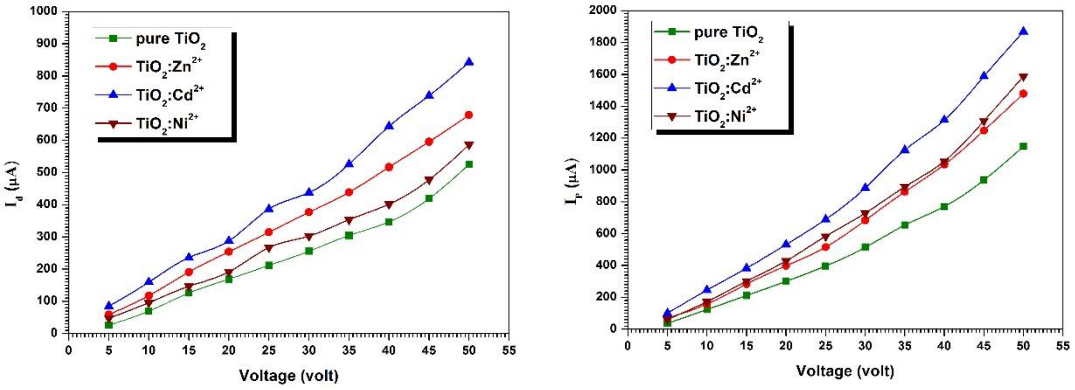


**Figure 6: Variation of photo and dark current for Pure , $Zn^{2+}$, $Cd^{2+}$and $Ni^{2+}$ doped $TiO_2$nano crystals.**

From the figures it reveals that the dark and photo currents for doped ($Zn^{2+}$, $Cd^{2+}$ and $Ni^{2+}$) $TiO_2$ nanocrystals are higher than that of pure $TiO_2$ nanocrystals. In all the doped $TiO_2$ ($TiO_2$:$Zn^{2+}$, $TiO_2$:$Cd^{2+}$ and $TiO_2$:$Ni^{2+}$) nanocrystals, photo currents are increased by two orders when compared to its corresponding dark current. However at higher applied electric filed it is increased by three orders. After doping of $Zn^{2+}$, $Cd^{2+}$ and $Ni^{2+}$, dark-conductivity in doped $TiO_2$ increases due to increase in thermally activated free carriers released from defect states introduced by incorporation of $Zn^{2+}$, $Cd^{2+}$ and $Ni^{2+}$ inside the $TiO_2$ nanocrystals.

The time-resolved rise and decay of photocurrent spectra's were recorded for pure and doped $TiO_2$ nanocrystals. Two sources with different illumination intensity of light are used to record the spectra. The prepared nanocrystals for photoconductivity measurement are first illuminated by Hg bulb of 300 W (treated as low intensity) for 45 min under visible lightwith constant dc field (30 V) then the light is switched off. The variation of photocurrent was measured with time in steps of every 20 seconds at room temperature. The similar procedure is repeated to measure the photo currents for all the samples illuminated by 600 watt Hg bulb (2 x 300 watt bulb)

(treated as high intensity). The time-resolved rise and decay of photocurrent spectra for undoped as well as different doped($Zn^{2+}$, $Cd^{2+}$ and $Ni^{2+}$)$TiO_2$nanocrystals are shown in Figures 7.

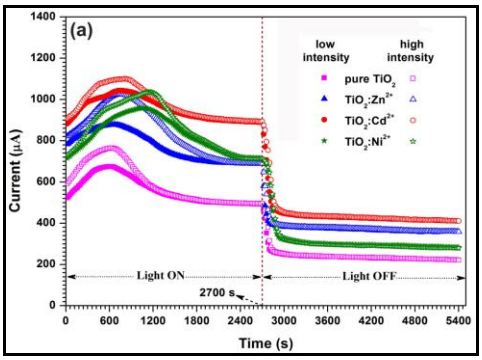


**Figure 7: Variation of time resolved rise and decay of photocurrent with different light intensity spectra of pure and doped $TiO_2$ nanocrystals**

It reveals that, under steady state illumination (in both the low and high intensity condition),all the nanocrystals (considered in the present study) exhibit anomalous behaviour. Such anomalous behavior was reported in ZnO nanowire, co-doped ZnO nanobelts etc.[19-21]. All the nanocrystals (pure and doped $TiO_2$) exhibit an increase in photocurrent during illumination up to few hundred seconds and attain a maximum value. This is due to fast process of generation of electron–hole pairs as a result of absorption of photons.After attaining maximum value of photocurrent it start decaying (anomalous behavior of photocurrent) even during steady illumination. This is caused by the presence of imperfection centers in the forbidden gap [22]of the pure and doped ($TiO_2$:$Zn^{2+}$, $TiO_2$:$Cd^{2+}$ and $TiO_2$:$Ni^{2+}$) $TiO_2$ nanocrystals. The addition of dopant ($Zn^{2+}$, $Cd^{2+}$ and $Ni^{2+}$)in the host $TiO_2$ lattice increases the photocurrent than the pure $TiO_2$ nanocrystals. In our case $Cd^{2+}$ doped $TiO_2$nanocrystals produces more photocurrent than the other doped ($TiO_2$:$Zn^{2+}$ and $TiO_2$:$Ni^{2+}$) $TiO_2$ nanocrystals. This is due to the illumination of light intensity in $TiO_2$:$Cd^{2+}$ nanocrystal produces more electron-hole pairs than that of the other doped nanocrystals. When illumination is switched off, the photocurrent decreases exponentially with in few ten seconds and attains a constantvalue for long time. This is due to the electrons recombine with holes and is captured by re-adsorbed oxygen molecules[23-24].

## 4. Conclusion

Pure and $Zn^{2+}$, $Cd^{2+}$ and $Ni^{2+}$ TiO2 quantum dots were prepared by simple solvothermal method. In our preparation technique the formation of oxygen defects at grain boundary region is very low, hence even at doped condition anatase phase of $TiO_2$ is formed. Our simple microwave irradiated solvothermal technique prevents the phase transformation of $TiO_2$ under annealing condition up to or less than 800 ºC. Our synthesis technique yielded highly pure and lesser crystallite size of $TiO_2$nanocrystals.From UV band gap calculation the dopant addition varies the band gap from 3.204 eV to maximum 3.556 eV, it suggest that the variation in energy band gap will be suitable for window material for fabrication of solar cells. The pure and doped $TiO_2$ nanocrystals have remarkable absorption in visible light region with a wavelength above 400 nm. The result indicates that the ability of prepared nanocrystals (considered in the present study) to harvest the visible component of solar radiation. Thus the prepared materials could be promising photo catalysts under visible light.

## 5. References

1. Ouyang M, Bai R, Yang L G, Chen Q , Han Y.G, Wang M, Yang Y, Chen HZ, High photoconductive vertically oriented $TiO_2$ nanotube arrays and their composites with copper phthalocyanine, J. Phys. Chem. C , 2008, 112, 2343–2348.
2. Adachi M , Murata Y, Takao J , Jiu J T, Sakamoto M , Wang F M, Highly efficient dye-sensitized solar cells with a titania thin-film electrode composed of a network structure of single-crystal-like TiO2 nanowires made by the “oriented attachment” mechanism, J. Am. Chem. Soc., 2004, 126, 14943–14949.

3. Jiu J T, Isoda S, Wang F M, Adachi M, Dye-sensitized solar cells based on a single-crystalline TiO2 nanorod film, J. Phys. Chem. B , 2006 , 110, 2087–2092.
4. Dholam R, Patel N, Adami M , Miotello A , Int J Hydrogen Energy, 2008, 33, 6896–6903.
5. Wang C, Ao Y H , Wang P F , Hou J ,Qian J , Mater Lett , 2010, 64, 1003–1006.
6. Patsoura A, Kondarides D I, Verykios X E, CatalToday , 2007, 124, 94–102.
7. Vitiello R P, Macak J M , Ghicov A, Tsuchiya H, Dick L F P, Schmuki P, N-doping of anodic TiO2 nanotubes using heat treatment in ammonia, Electrochem. Commun., 2006, 8, 544–548.
8. Khan M A, Akhtar, M S, Woo S I,Yang O B, Enhanced photoresponse under visible light in Pt ionized TiO2 nanotube for the photocatalytic splitting of water, Catal. Commun. 2008, 10,1–5.
9. Paulose M, Shankar K, Varghese O K, Mor G K, Grimes C A, Application of highly-ordered $TiO_2$ nanotube arrays in heterojunction dye-sensitized solar cells, J. Phys. D: Appl. Phys., 2006, 39, 2498–2503.
10. Hsu M C, Leu I C, Sun Y M, Hon M H, Fabrication of CdS@$TiO_2$ coaxial composite nanocables arrays by liquid-phase deposition, J. Cryst. Growth 2005, 285, 642–648.
11. Chen W, Qi D, Surface transfer doping of semiconductors, Progress in Surface Science, 2009, 84, 279.
12. Liu J ,Yang H T, Tan WW, Zhou XW, Lin Y Photovoltaic performance improvement of dye-sensitized solar cells based on tantalum-doped TiO2 thin films, ElectrochimicaActa,2010, 56, 396.
13. Suwanboon S, Amornpitoksuk P, Bangrak P, Synthesis, characterization and optical properties of Zn1-xTixO nanoparticles prepared via a high-energy ball milling technique. Ceram Int., 2011, 37, 333- 340.
14. Tauc J, Grigorovici R, Vancu A, Optical properties and electronic structure of amorphous Germanium, Phys. Status Solidi b, 1966,15, 627–637.
15. Yin W J , Chen S, Yang J H, Gong X G, Yan Y , Wei S H, Effective band gap narrowing of anatase $TiO_2$ by strain along a soft crystal direction, Applied Physics Letters, 2010,96, 221901-3.
16. Ilican S, Caglar M , Caglar Y , Determination of the thickness and optical constants of transparent indium-doped ZnO thin films by the envelope method, Materials Science – Poland, 2007, 25,709-718.
17. Zhao Y, Li C Z, Liu X H, Gu F, Jiang H B, Shao W , Zhang L, He Y, Mater. Lett. , 2007, 61 ,79.
18. Joshi VN, Photoconductivity, 1990, Marcel Dekker, New York.
19. Ahn S E , Ji H J, Kim K , Kim G T , Bae C H, Park S M, Kim Y K, Ha J S, Appl. Phys.Lett. , 2007, 90, 153106.
20. Peng L, Zhai J L, Wang D J, Wang P, Zhang Y, Pang S , Xie T F, Chem. Phys. Lett. , 2008, 456, 231.
21. Bera A, Basak D, Appl. Phys. Lett., 2009, 94, 163119.
22. Devi S , Prakash S G, J. Ind. Pure Appl. Phys., 1995, 33, 319.
23. Liao Z M, Xu J, Zhang J M, Yu D P, Appl. Phys. Lett. ,2008, 93, 023111.
24. Zheng X G, Sh Q. Li, Hu W, Chen D, Zhang N, Shi M J, Wang J J, Zhang Ch L, J. Lumin., 122, 198, 2007.

*****